Charged Pion Electroproduction Ratios

Detection Efficiency Studies

Argha Das

arghadas0001@gmail.com

June 28, 2025

Introduction:

This project aims to analyze charged pion electroproduction data obtained from the liquid deuterium (LD_2 target at Jefferson Lab. The focus has been on data analysis on plots of LD_2^+ and LD_2^- datasets using ROOT. The work involves applying various detector cuts, such as those on missing mass versus other detectors, to isolate the signals corresponding to pions. With the LD_2^- data, additional attention was given to applying extra cuts to remove electron contamination while ensuring the pion signal remains consistent with the LD_2^+ analysis. The SHMS focal plane includes Aerogel Cherenkov Detector, Heavy Gas Cherenkov Detector, Noble Gas Cherenkov Detector, Lead-Glass Shower Calorimeter, Scintillator Hodoscopes, and Drift Chambers. The HMS focal plane includes Gas Cherenkov Detector, Hodoscopes, Drift Chambers and Lead-Glass Shower Calorimeter. These detectors play an essential role in particle identification and event selection. This progress report outlines the methodologies and the results achieved so far.

Data analysis was done using ROOT. The run list for the LD_2^+ setting is 15091 to 15094. It is essential to isolate π^+ particles from the LD_2^+ setting, which provides a greater insight into the cuts required for π^- particles for the LD_2^- setting.

Methodology:

To isolate charged pion events from the LD_2^+ and LD_2^- datasets, a series of cuts was applied based on both timing and particle identification (PID) criteria. These cuts were chosen based on the characteristics of the detectors within the High Momentum Spectrometer (HMS) and Super High Momentum Spectrometer (SHMS) focal planes. Each detector played a specific role in identifying particle types and eliminating background events such as electrons, positrons, protons, and kaons.

The coincidence time (Coin Time) measures the time difference between signals in the two spectrometers (SHMS and HMS) arms. A sharp peak in this distribution indicates prompt events, such as the detection of a pion and an electron in coincidence. The RF time reflects how well an event aligns with the known timing structure of the accelerator beam, which is clustered at a fixed frequency. Events within the beam's time window are more likely to be true physics events. In plots of missing mass vs. RF time, real pion events cluster in a well-defined band. The HMS calorimeter is an electromagnetic calorimeter that measures energy deposited by a particle and normalizes it to the particle's momentum. Electrons and positrons deposit nearly all of their energy, producing normalized values close to 1.0, while hadrons, including pions, deposit less, resulting in a value lower than 1.0. The HMS Heavy Gas Cherenkov detector identifies particles that emit Cherenkov light when travelling faster than the speed of light in a given medium, also known as the threshold velocity. Pions at relevant momenta produce Cherenkov light and generate photoelectrons. The HMS is the electron arm, so the detector's main job is to positively tag the scattered electron and reject hadrons that occasionally enter the HMS acceptance.
In contrast, slower particles like protons and kaons typically produce much less Cherenkov light and photoelectrons. The SHMS calorimeter, similar to its HMS counterpart, is used for

electron/hadron discrimination. In the LD_2^- setting, electrons are a significant source of background and appear near normalized values of 1.0. The SHMS Noble Gas Cherenkov detector is used to detect high-speed particles, such as electrons, which emit large amounts of Cherenkov light in its low-density gas. Pions, being heavier than electrons, produce less Cherenkov light and photoelectrons than electrons.

LD_2^+ Analysis:

Initially, an important variable called coin-time (ePiCoinTime_ROC1) was used to eliminate unnecessary background noise; the prominent peak in the Coin-time distribution was also shifted to zero for improved visualization.

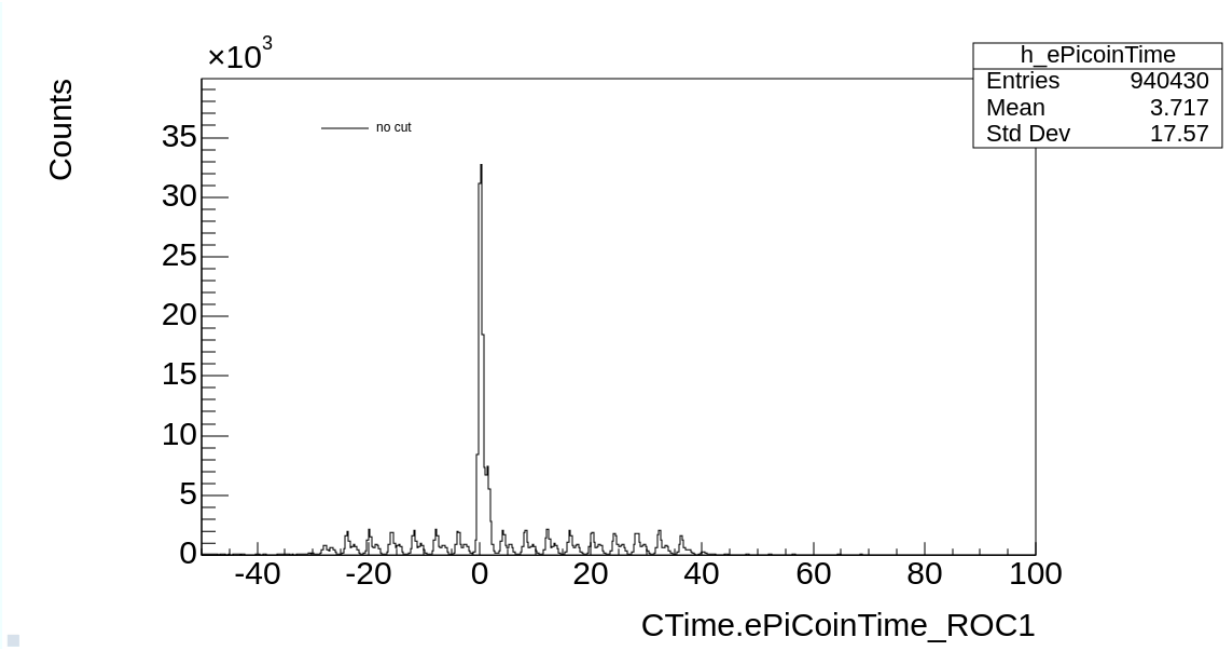

(Figure 1.0)

Figure 1.0 represents the Coincidence time plot. Coincidence time refers to the difference in arrival times between two detected particles, measured between detectors placed in different arms of the spectrometer (like HMS and SHMS). The prominent central peak in Figure 1.0

corresponds to the prompt pions. Prompt pions are produced simultaneously with the scattered electron during a single interaction between the incident electron beam and the target nucleon. As such, they will arrive at the detectors within a narrow, well-defined time window relative to the scattered electron. Selecting prompt pions allows for the rejection of accidental or random coincidences, which improves the signal-to-noise ratio and ensures that only events corresponding to real pion production are chosen. Random peaks from events less than -0.8 and greater than 2.2 correspond to unrelated or random background events irrelevant to this analysis. Furthermore, the secondary peak around count 8 represents heavier particles than pions, such as Kaons and protons. It is crucial to apply cuts around the central peak to select present events to remove the background. Moreover, it is necessary to use cuts to get rid of that secondary peak around 0.7 nanoseconds (ns) to 1.9 ns, to get rid of those kaons and protons, as well as the smaller background peaks.

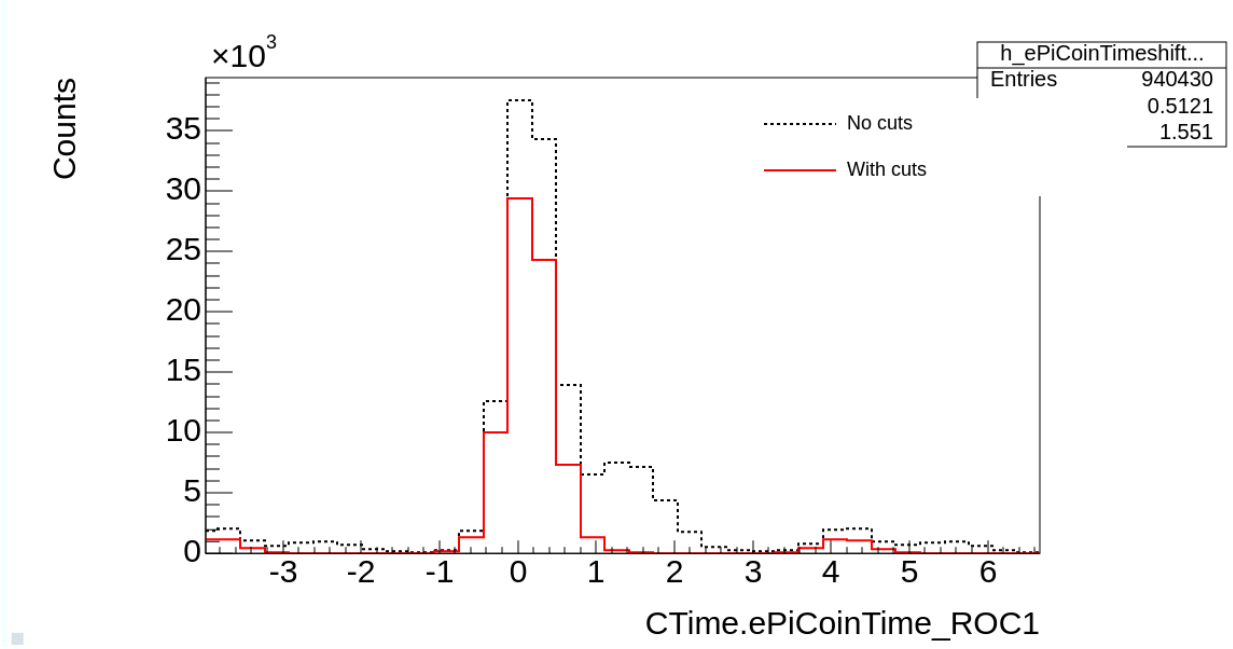

(Figure 2.0)

The cuts are applied to the coin-time were:

SHMS Aerogel (P.aero.npeSum) > 2.0

SHMS Heavy Gas (P.hgcer.npeSum) > 2.0

HMS Calorimeter (H.cal.etottracknorm) > 0.7,

HMS Heavy Gas (H.cer.npeSum) > 2.0.

The cuts produced the coin-time plot in Figure 2.0, which is zoomed in compared to Figure 1.0. The applied cuts successfully isolated the large peak, removed the secondary peak as intended, and removed those small peaks, which led to a cut of -2.0 ns < Coin-Time < 2.0 ns. This cointime cut was applied to all the plots in the data analysis to isolate π^+.

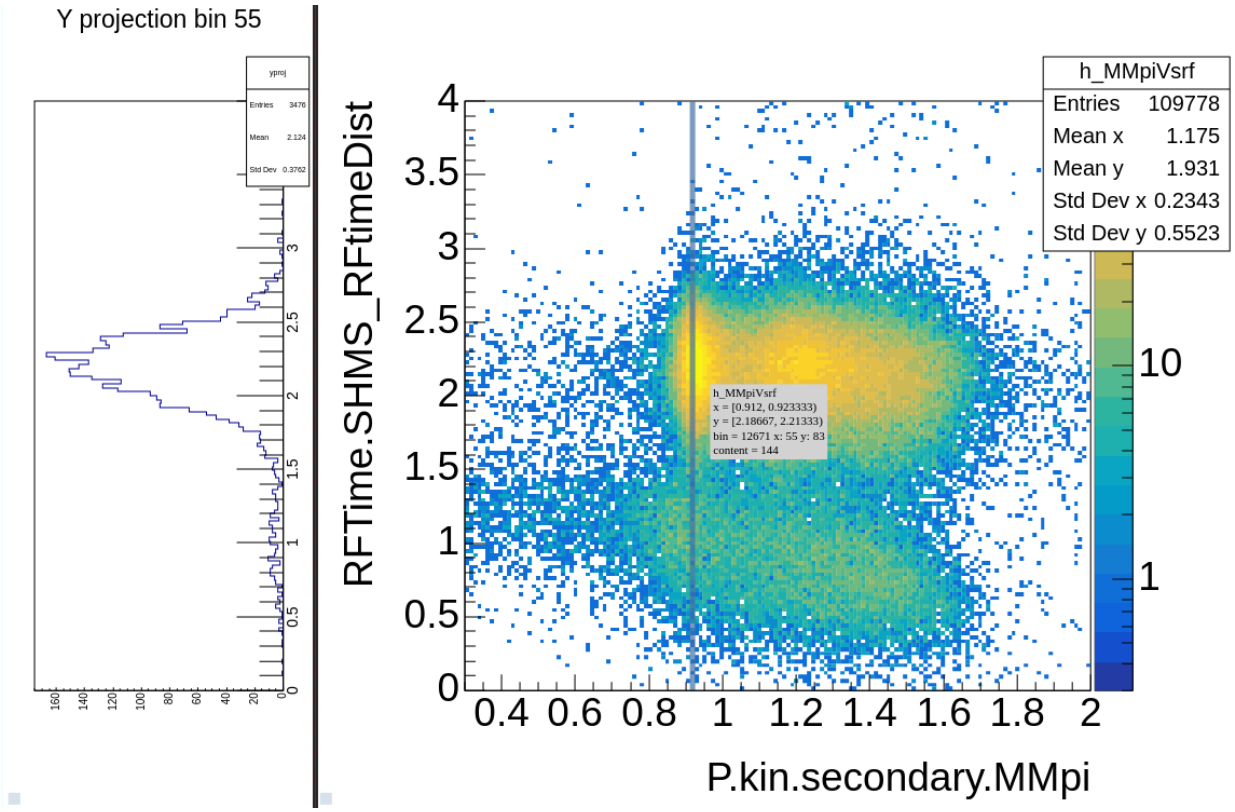

(Figure 3.0)

Another cut, the RF-time (RFTime.SHMS_RFtimeDist), was used after the coin time cut was applied to all the plots. RF time provides the phase of the detected particle relative to the electron bunches in the accelerator beam. Figure 3.0 is generated using the missing mass of the

pion (MMpi, x-axis) versus RF time (y-axis). Missing mass (MM) refers to the mass of the undetected particle inferred from conservation of energy and momentum. It is instrumental in reactions where the final-state particles are not directly observed. In the context of charged pion electroproduction, the missing mass is used to identify the nucleon (e.g., a neutron or proton) by analyzing the kinematics of the detected scattered electron and produced pion.

The missing mass (MM) is defined through the four‑momentum balance of the reaction:

$$e + P \longrightarrow e' + \pi + N$$

(Figure 4.0)

- e: incoming electron
- P: proton at rest
- e′: Scattered electron
- π: pion
- N: Neutron

Writing out the invariant mass equation ($E^2 - p^2 = MM^2$) in terms of energy and three-momentum components will lead to this equation.

$$MM^2 = (E_e + E_P - E_{e'} - E_\pi)^2 - (p_e + p_P - p_{e'} - p_\pi)^2$$

(Figure 5.0)

- E_e: energy of the incoming electron
- E_P: energy of the proton
- $E_{e'}$: energy of the scattered electron
- E_π: energy of the detected pion

- p_e: momentum of the incoming electron
- p_P: momentum of the proton
- $p_{e'}$: momentum of the scattered electron
- p_π: momentum of the detected pion

The equation in Figure 5.0 suggests that the missing mass is equivalent to the neutron mass of 0.937 $\frac{GeV}{c^2}$. When the missing mass equals the known neutron mass, it indicates that the undetected particle in the reaction is a neutron and no additional particles were produced in the final state. Plotting the missing mass distribution and observing a sharp peak at approximately 0.937 $\frac{GeV}{c^2}$ allows for the selection of exclusive π events. Therefore, applying cuts around 0.937 $\frac{GeV}{c^2}$ in the missing mass versus other detector plots ensures that only events consistent with pion production and a single recoil neutron are retained, significantly improving the purity and accuracy of the analysis.

The most prominent events in Figure 3.0 appear within the range of 1.5 to 3.1. The events below 1.5 are protons, leading to the conclusion that 1.5 < RFtime < 3.0 cut, which was applied to all the other plots.

After some iterations and comprehensive analysis of all the MMpi plots compared to other detectors, it was concluded that the applied cuts were not only appropriate but also necessary. These cuts were consistently applied to all the plots in the data analysis, ensuring the validity and reliability of our findings.

-2.0 < Coin Time (CTime.ePiCoinTime_ROC1) < 2.0

1.5 < RFtime (RFTime.SHMS_RFtimeDist) < 3.0

HMS Calorimeter (H.cal.etottracknorm) > 0.7

HMS Heavy Gas (H.cer.npeSum) > 2.0

SHMS Calorimeter (P.cal.etottracknorm) < 0.8

SHMS Noble Gas (P.ngcer.npeSum) < 2.4

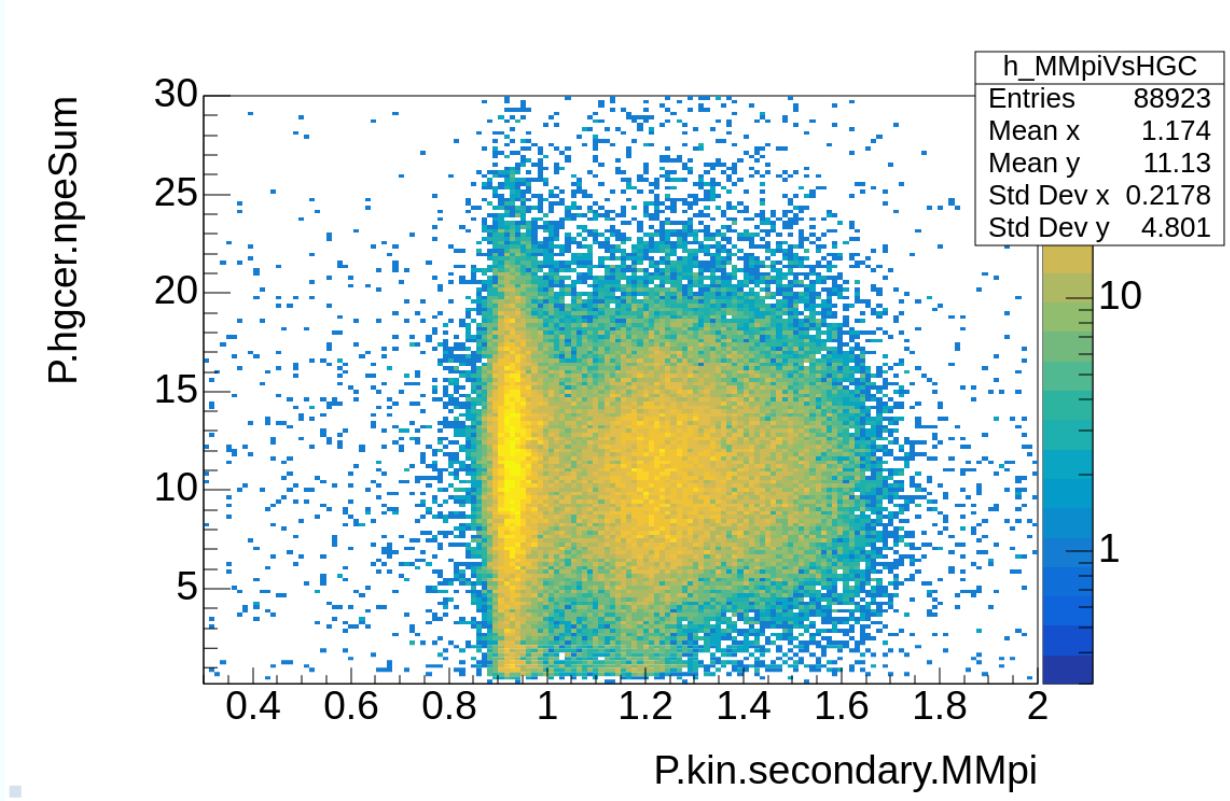

(Figure 6.0)

Figure 6.0 is MMπ (x-axis) vs SHMS Heavy Gas Cherenkov detector (y-axis). The initial cut chosen for the SHMS Heavy Gas Cherenkov detector was P.hgcer.npeSum > 0.5. However, this cut was ultimately eliminated from all the other plots because the detector showed minimal background noise in the π region (low npeSum values), meaning that few unwanted particles, such as electrons or protons, are present within that range. This low background at small npeSum occurs because kaons, being below the heavy-gas Cherenkov threshold, produce few Cherenkov

light in this radiator; therefore, any remaining hits in that region are overwhelmingly true π events. Furthermore, in Figure 6.0, there is a significant increase in background noise above the y-value of 5. The strong rise at large P.hgcer.npeSum reflects lepton contamination (positrons in LD_2^+, electrons in LD_2^-), which are well above the heavy-gas Cherenkov threshold and therefore yield many photoelectrons. This lepton band drives the high-missing-mass background, whereas kaons and protons are typically below threshold in this detector and do not account for the high P.hgcer.npeSum events. Due to coincidence-time and RF-time cuts, the majority of the heavier particle events are cut. Applying the SHMS Heavy Gas Cherenkov detector cuts barely added an improvement to the signal purity while risking the loss of π near the threshold.

In addition, SHMS Aerogel Cherenkov detector cuts were also excluded from all plots due to the effectiveness of the previously applied cuts. As discussed in the analysis of Figure 2.0, the secondary peak from approximately 0.9 to 2.6 corresponds to heavier particles, such as kaons and protons.

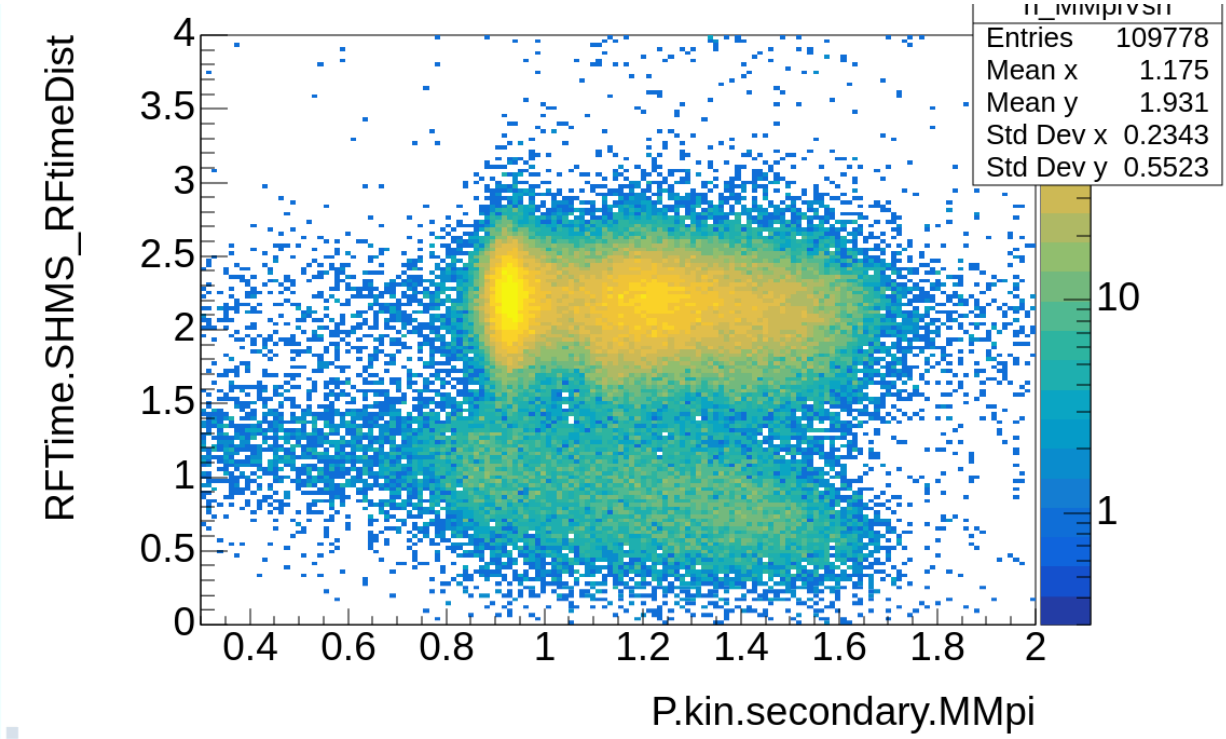

(Figure 7.0)

Furthermore, the events in Figure 7.0 below 1.5 on the y-axis correspond to protons when examining the RF time plot. These proton events were eliminated since the RF time cuts in Figure 3.0 were above the y-value of 1.5. Although the Aerogel detector cut is suitable for proton rejection, it is not necessary to include it in the final data analysis, since it will have barely any improvement.

LD_2^- Analysis

All the data above are for isolating π^+; the data analysis was done in the LD_2^+ setting. However, the LD_2^- setting introduces additional electron background, which must be eliminated with various cuts. Additionally, the plots generated in LD_2^- after the necessary cuts should look similar to the plots in LD_2^+ setting. For the LD_2^- setting, the goal is to isolate π^-; the run list for

the LD_2^- setting is from 15985 to 15988. Moreover, the cuts in the LD_2^- setting are made in comparison to the LD_2^+ setting.

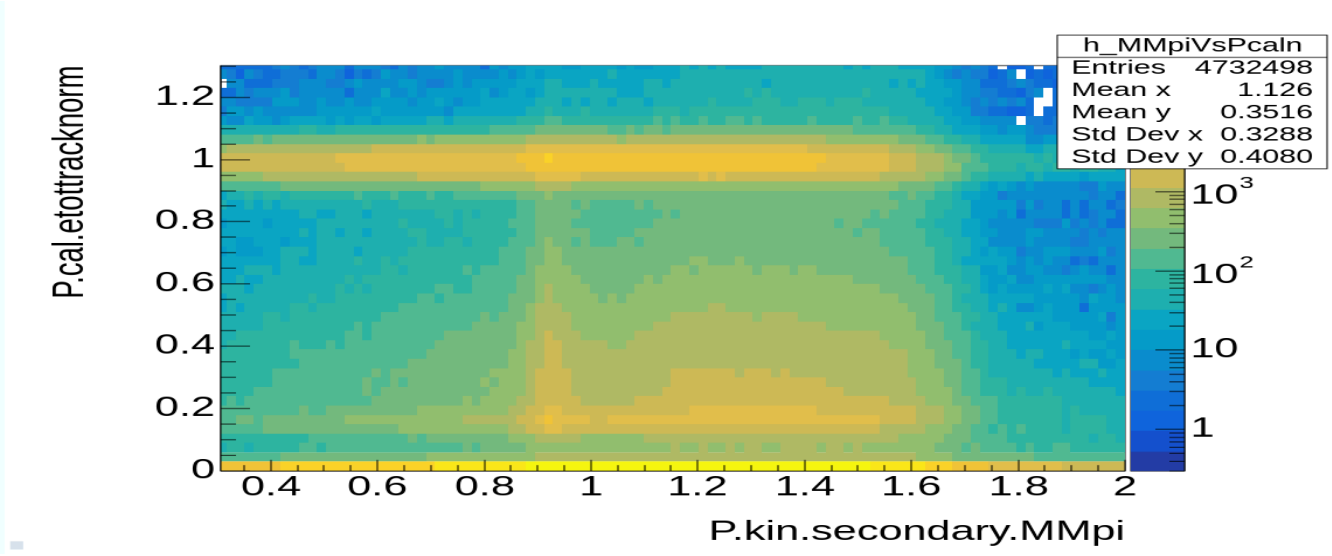

(Figure 8.0)

Figure 8.0 is generated in the LD_2^- setting and represents the MMπ vs. SHMS Calorimeter detector (P.cal.etottracknorm). The SHMS Calorimeter cuts do not significantly impact plots/data for the LD_2^+ setting; this is because LD_2^+ consists of only a few positrons, with the positive hadrons (that do not give a large signal in the calorimeter) dominating; furthermore, positrons are only a small portion of the positive particle flux, while electrons constitute a significant portion of the negative flux; the LD_2^- setting is dominated by electrons. Thus, the SHMS Calorimeter cut is significant to the LD_2^-, to get rid of as many electrons as possible. In Figure 8.0, the horizontal line around one at the y-axis at a y-value of approximately 1.0 represents electrons, so the SHMS calorimeter has to be less than 1. At the end, the appropriate cut chosen for the SHMS calorimeter detector was P.cal.etottracknorm < 0.8. After applying all the necessary cuts, this plot is expected to resemble the corresponding MMπ vs. SHMS Calorimeter detector (P.cal.etottracknorm) plot in the LD_2^+ setting in Figure 9.0.

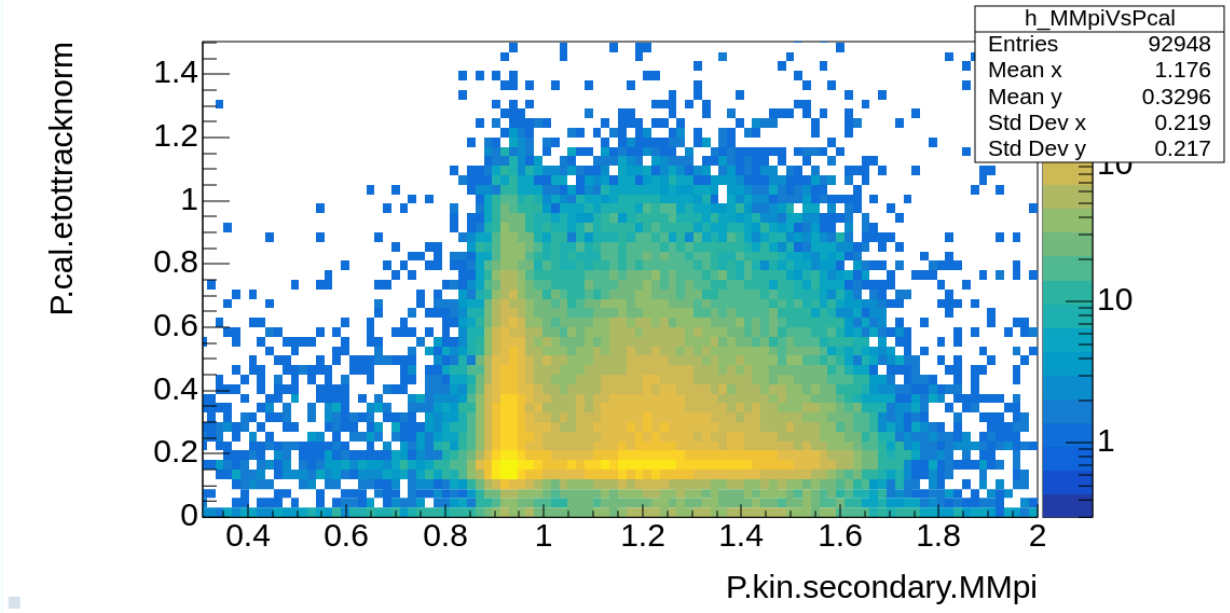
h_MMpiVsPcal
Entries 92948
Mean x 1.176
Mean y 0.3296
Std Dev x 0.219
Std Dev y 0.217
P.cal.etottracknorm
P.kin.secondary.MMpi
0
0.2
0.4
0.6
0.8
1
1.2
1.4
0.4
0.6
0.8
1
1.2
1.4
1.6
1.8
2
10
1

(Figure 9.0)

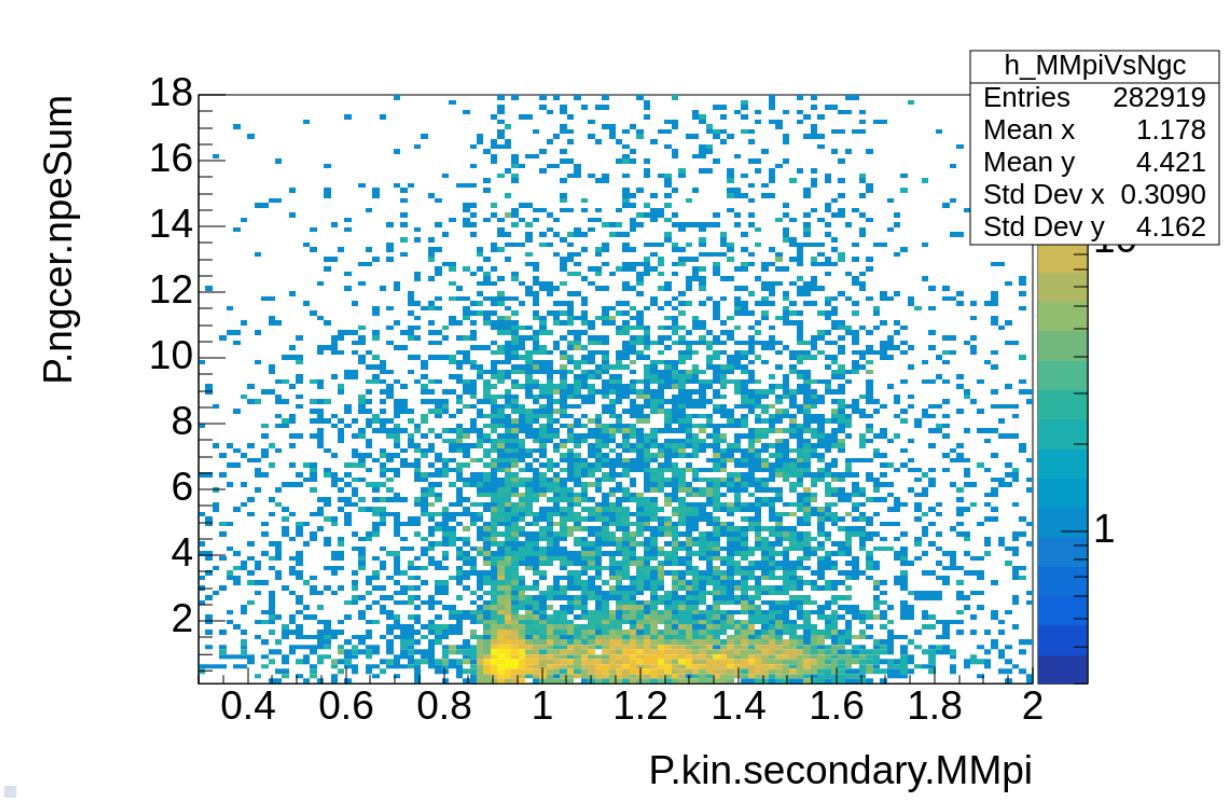

(Figure 10.0)

Another plot important to the LD_2^- setting involves the SHMS Noble Gas Cherenkov detector. The plot in Figure 10.0 represents MMπ vs. SHMS Noble Gas (P.ngcer.npeSum) in the LD_2^- setting. Like the SHMS Calorimeter, the Noble Gas Cherenkov cut does not significantly impact the LD_2^+ setting, as that setting contains positrons rather than electrons. Due to the LD_2^- setting being dominated by electrons, the SHMS Noble Gas Cherenkov detector becomes prominent at getting rid of electrons from the plots within the LD_2^- . Most of the signals for pions in Figure 10.0 are less than 3, but when considering a stricter cut for SHMS Noble Gas, it is helpful to examine the SHMS Noble Gas versus SHMS Calorimeter plot.

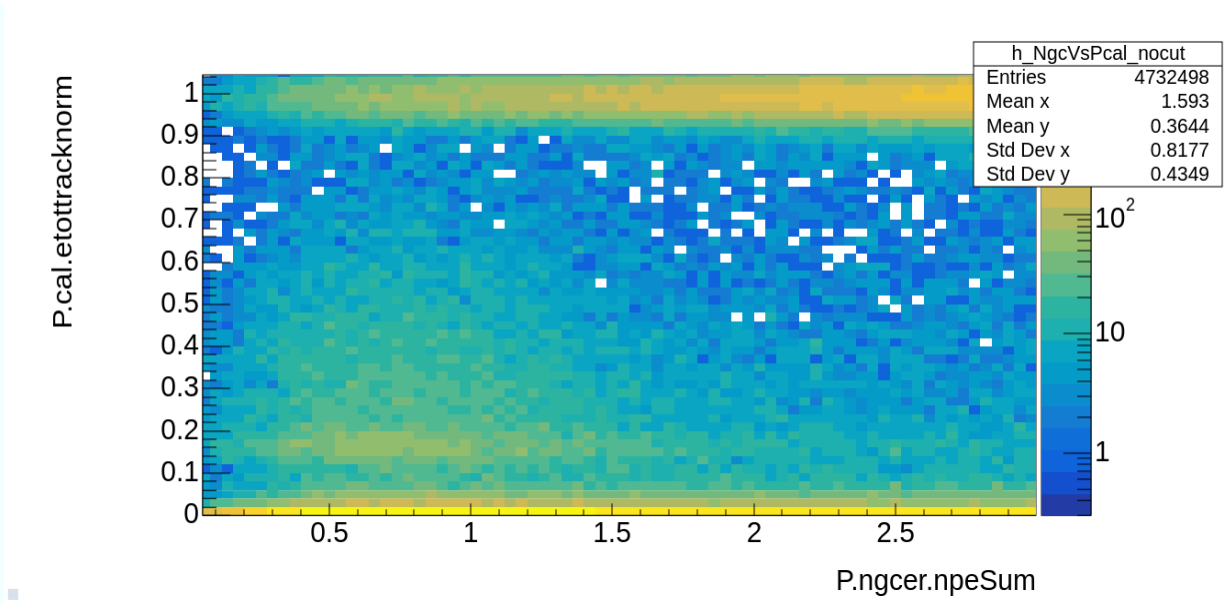

(Figure 11.0)

Figure 11.0 (LD_2^-): SHMS Noble Gas Cherenkov (x-axis) vs. SHMS Calorimeter (y-axis) for the LD_2^- dataset. This plot is used to determine the appropriate cut for the SHMS Noble Gas detector in order to isolate π^- events. The distinct band of high-density events in the upper portion of the plot corresponds to electrons, which deposit more energy in the calorimeter and produce higher photoelectron counts in the Cherenkov detector. In contrast, hadrons such as pions cluster in the lower portion of the plot, showing lower responses in both detectors. The white region near x = 2.4 represents the visual gap between these two populations, electrons above and hadrons below, and is where the separation between them becomes most apparent. Based on this separation, the cut P.ngcer.npeSum < 2.4 was chosen to reject electrons while preserving π^- events effectively.

The HMS cuts from the LD_2^+ setting were retained for the LD_2^- setting, as they do not significantly impact the LD_2^- data compared to the SHMS cuts. Similarly, the coincidence time cut for the LD_2^- setting remained unchanged. This consistency is due to the effectiveness of the previously applied cuts, such as:

1.5 < RFtime (RFTime.SHMS_RFtimeDist) < 3.0

HMS Calorimeter (H.cal.etottracknorm) > 0.7

HMS Heavy Gas (H.cer.npeSum) > 2.0

SHMS Calorimeter (P.cal.etottracknorm) < 0.8

SHMS Noble Gas (P.ngcer.npeSum) < 2.4

-2 < coin time < 2, cut was fine to proceed with, as we got rid of the background noise showcased in Figure 12.0.

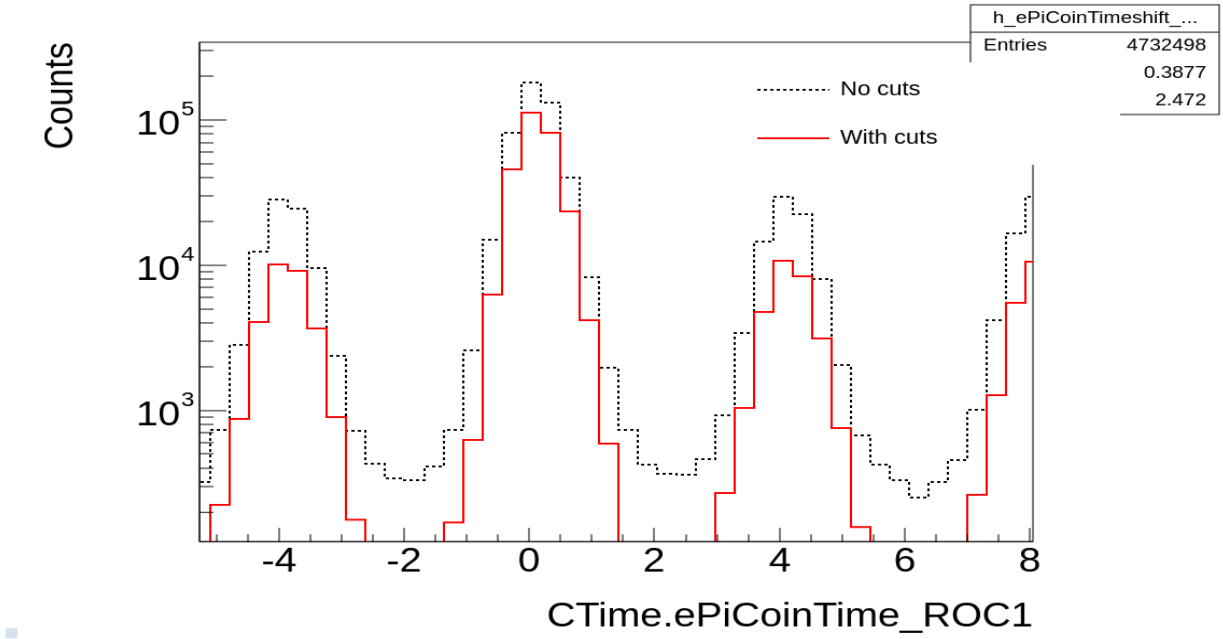

(Figure 12.0)

Results:

In this section, results for all the plots will be provided. The plots will be placed adjacent to each other. The left side is the uncut version of the plot, and the right side is when these cuts are applied:

-2.0 < Coin Time (CTime.ePiCoinTime_ROC1) < 2.0

1.5 < RFtime (RFTime.SHMS_RFtimeDist) < 3.0

HMS Calorimeter (H.cal.etottracknorm) > 0.7

HMS Heavy Gas (H.cer.npeSum) > 2.0

SHMS Calorimeter (P.cal.etottracknorm) < 0.8

SHMS Noble Gas (P.ngcer.npeSum) < 2.4

(Figure 13.0)

It is important to emphasize that the cuts applied to the LD_2^- data were made in direct comparison to the LD_2^+ data. LD_2^+ consists of positively charged particles, including positrons, while LD_2^- has negatively charged particles, including electrons. Due to LD_2^- being electron-dominated, cuts from different detectors must be applied to get rid of the electrons. Despite these differences in charge and background composition, the pions in both LD_2^+ and LD_2^- originate from the same reactions and kinematic conditions. As a result, the π^+ in LD_2^+ and π^- in LD_2^- are expected to appear in the same regions. This means that plots from the LD_2^- setting should look very similar to the plots from the LD_2^+ setting after the appropriate cuts. Furthermore, when applying the cuts from Figure 13.0, the cuts from the same detector are not mentioned to avoid affecting the data.

For LD_2^+ plots:

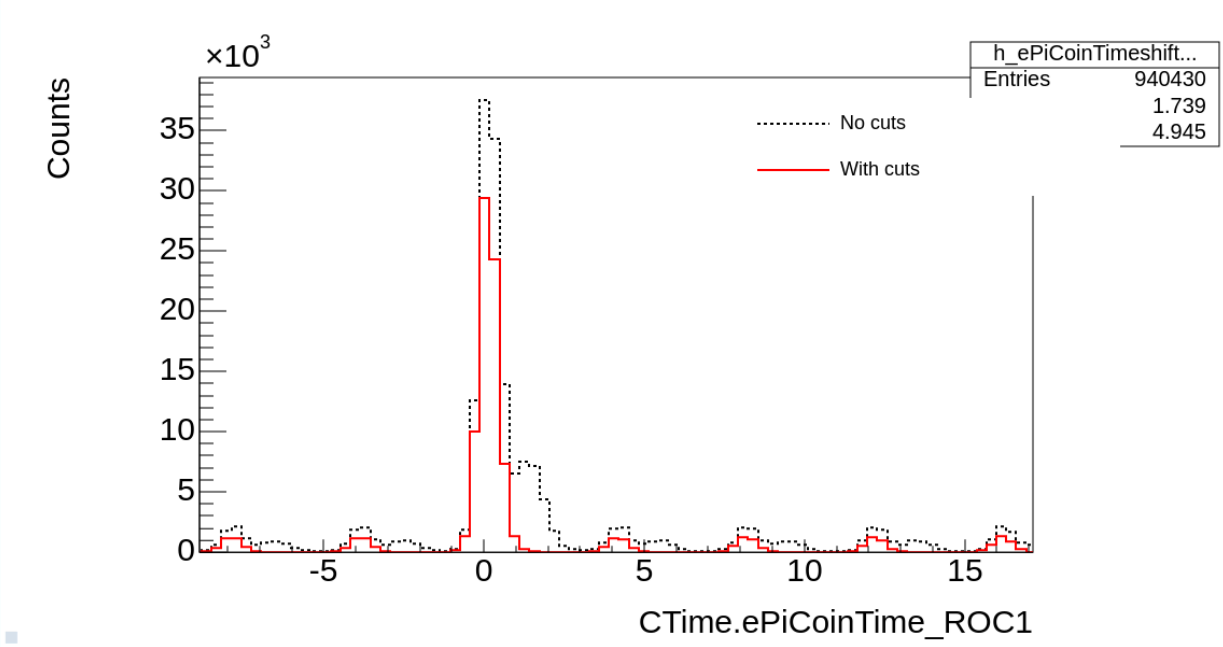

(Figure 14.0)

Figure 14.0 represents the coincidence time plot. Coincidence time refers to the difference in arrival times between two detected particles, measured between detectors placed in different arms of the spectrometer (like HMS and SHMS). The prominent central peak in Figure 14.0 corresponds to the prompt pions. Selecting prompt pions allows for the rejection of accidental or random coincidences, which improves the signal-to-noise ratio and ensures that only events corresponding to real pion production are chosen. Smaller peaks from events less than -0.8 and greater than 2.2 correspond to unrelated or random background events. The secondary peak around count 8 represents heavier particles than pions, such as Kaons and protons.

SHMS Aerogel (P.aero.npeSum) > 2.0

SHMS Heavy Gas (P.hgcer.npeSum) > 2.0

HMS Calorimeter (H.cal.etottracknorm) > 0.7,

HMS Heavy Gas (H.cer.npeSum) > 2.0.

The applied cuts successfully isolated the prominent peak and got rid of the secondary peak around 0.7 to 1.9, to get rid of those kaons and protons, as well as the smaller background peaks.

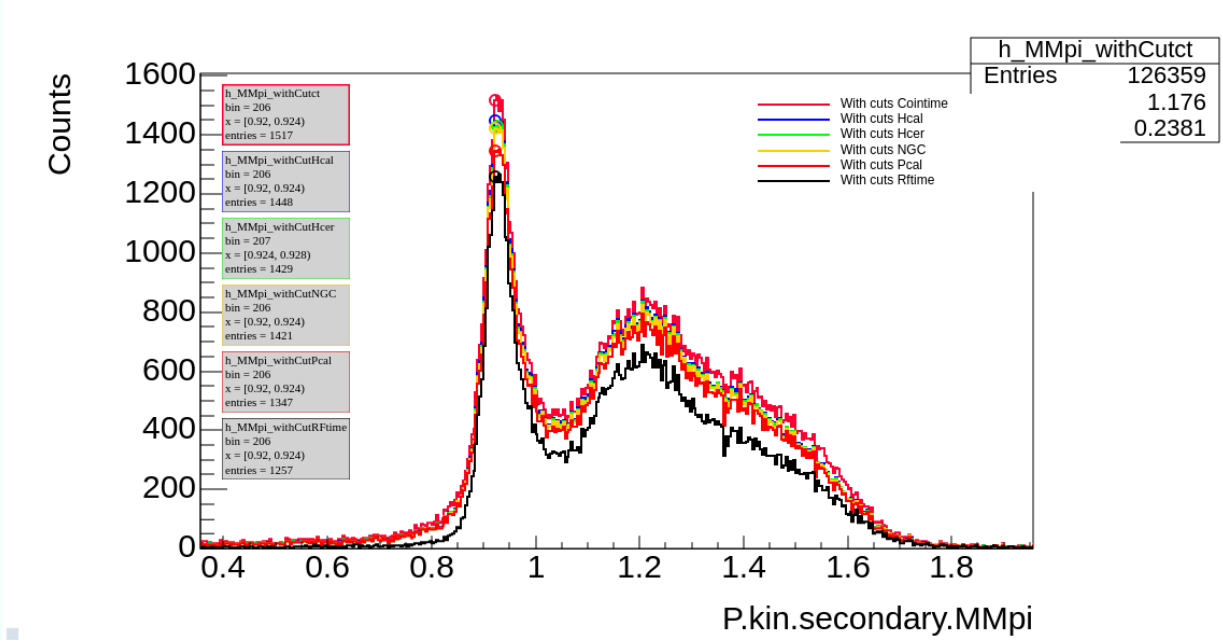

(Figure 15.0)

Figure 15.0 represents the Missing Mass of pions(MMπ) distribution plot in the LD_2^+ setting. Missing mass (MM) is the mass of the undetected particle, assuming the detected final-state particles are the scattered electron and π^+ . The x-axis is the missing mass in $\frac{GeV}{c^2}$, and the y-axis is the count (number of events). A sharp peak near 0.937 $\frac{GeV}{c^2}$ corresponds to the neutron mass, which validates the expected pion electroproduction process with a missing neutron in the final state. Each colored curve represents the effect of a specific cut on top of the previous cuts. The curve with black colouring has all the applied cuts and peaks at the neutron mass, with minimal background events.

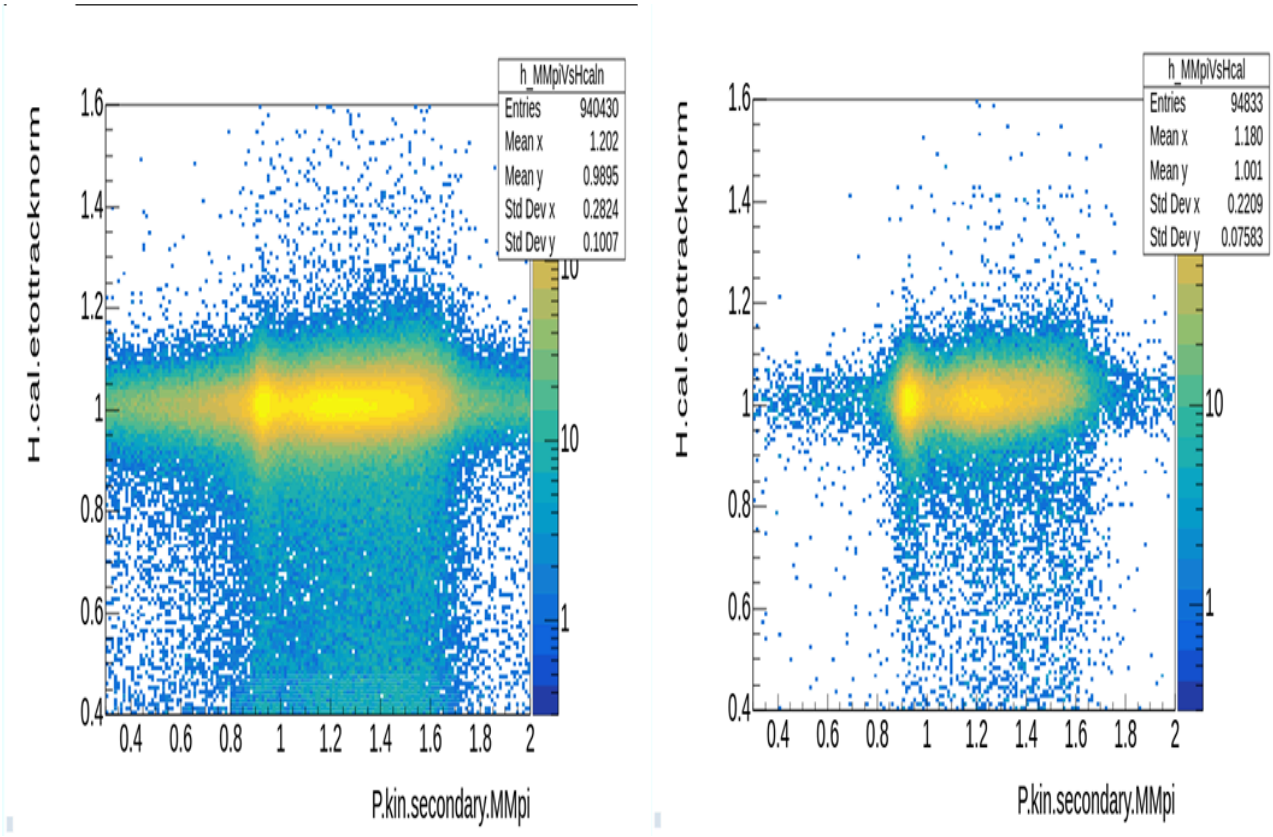

(Figure 16.0)

(a) (b)

Figure 16.0, panels a) and b), represent the MMπ versus HMS Calorimeter (H.cal.etottracknorm) plots in the LD_2^+ setting. Panel a) represents MMπ versus HMS Calorimeter plot without any cuts; panel b) showcases the plot with cuts from Figure 13.0. HMS Calorimeter (H.cal.etottracknorm) is excellent for electron vs hadron discrimination. However, due to the plot being within the LD_2^+ setting, rather than electrons, positrons are involved. Like electrons, positrons deposit nearly all of their energy in the calorimeter, resulting in a value of H.cal.etottracknorn of 1. In contrast, hadrons such as protons, kaons and pions deposit a smaller fraction of their energy in the calorimeter, which may result in the value from 0.5 to 0.8. To isolate the heavier particles like kaons and protons, and ensure the H.cal.etottracknorm cut is

closer to the neutron mass of 0.937 $\frac{GeV}{c^2}$, H.cal.etottracknorm > 0.7 was chosen to be applied to the rest of the cuts.

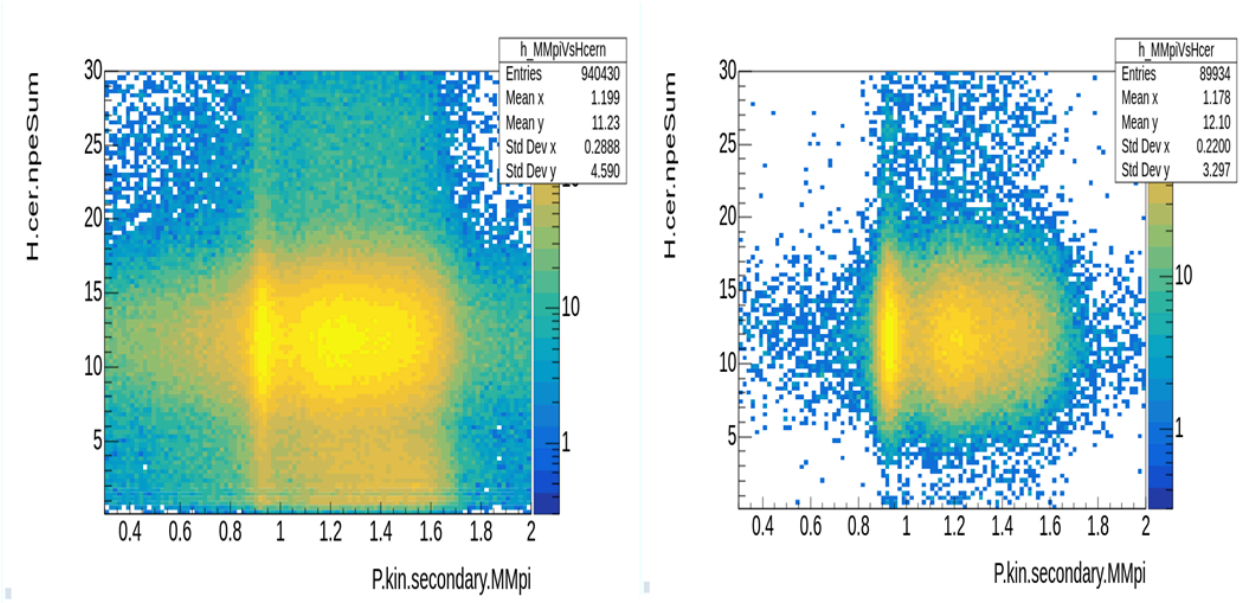

(Figure 17.0)

(a) (b)

Figure 17.0, panels a) and b), represent the MMπ versus HMS Heavy Gas Cherenkov detector (H.cer.npeSum) plots in the LD_2^+ setting. Panel a) represents MMπ versus HMS Heavy Gas Cherenkov detector plot without any cuts; panel b) showcases the plot with cuts from Figure 13.0. The HMS Heavy Gas Cherenkov detector is used for particle identification (PID). Heavier particles, such as protons and kaons, produce less Cherenkov light than pions due to them travelling slower than pions, which may lead to heavier particles producing H.cer.npeSum signals lower than 1.5. To isolate heavier particles and ensure the H.cer.npeSum signals are closer to the neutron mass of 0.937 $\frac{GeV}{c^2}$, H.cer.npeSum > 2.0 was chosen to retain pion events.

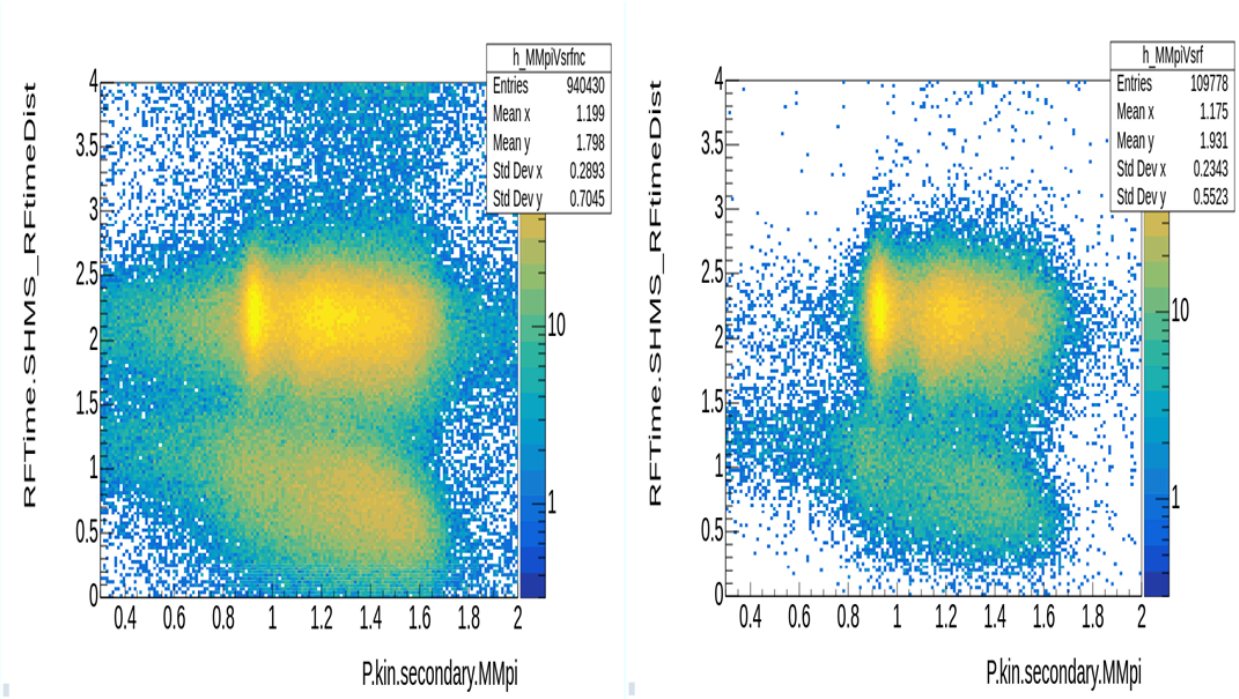

(Figure 18.0)

(a) (b)

Figure 18.0, panels a) and b), represent the MMπ versus RF-time (RFTime.SHMS_RFtimeDist) plots in the LD_2^+ setting. Panel a) represents MMπ versus RF-time plot without any cuts; panel b) showcases the plot with cuts from Figure 13.0. RF-time represents the timing of a detected particle relative to the electron beam's radio-frequency (RF) structure. RF-time helps determine whether a detected particle is in phase with the beam, meaning it likely originated from a true interaction event, or is out of phase, indicating a random or background hit. The events in Figure 18.0 Panel (b) below 1.5 on the y-axis correspond to protons, to isolate pions from the heavier particles, 1.5 < RFtime (RFTime.SHMS_RFtimeDist) < 3.0 cut was chosen, making sure the events are centred at the neutron mass (0.937 $\frac{GeV}{c^2}$), indicating successful selection of in-time pion events.

For LD_2^- plots:

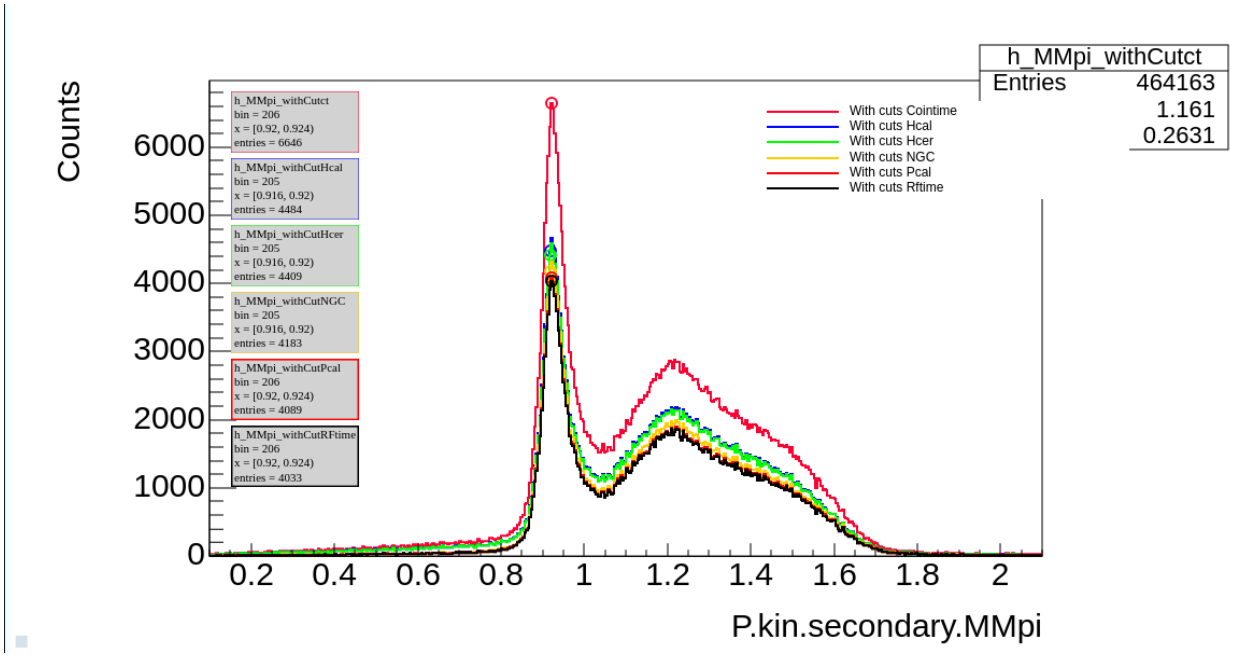

(Figure 21.0)

Figure 21.0 represents the Missing Mass of pions(MMπ) distribution plot in the LD_2^- setting. Missing mass (MM) is the mass of the undetected particle, assuming the detected final-state particles are the scattered electron and π^-. The x-axis is the missing mass in $\frac{GeV}{c^2}$, and the y-axis is the count (number of events). A sharp peak near 0.937 $\frac{GeV}{c^2}$ corresponds to the neutron mass, which validates the expected pion electroproduction process with a missing neutron in the final state. Each colored curve represents the effect of a specific cut on top of the previous cuts. The curve with black colouring has all the applied cuts and peaks at the neutron mass, with minimal background events.

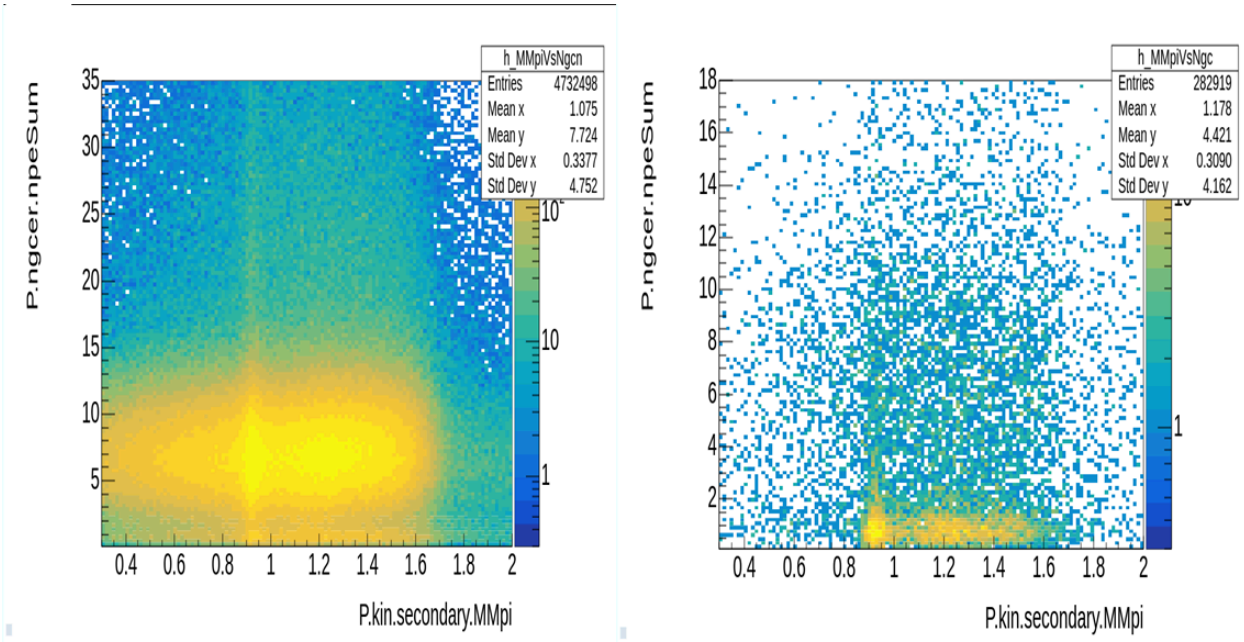

(Figure 22.0)

(a) (b)

Figure 22.0, panels a) and b), represent the MMπ vs. SHMS Noble Gas Cherenkov detector (P.ngcer.npeSum) plots in the LD_2^- setting. The SHMS Noble Gas Cherenkov detector is filled with low-density gas, which means particles with a certain velocity threshold (exceeding the speed of light within a particular medium) will emit Cherenkov light. The number of photoelectrons produced in the SHMS Noble Gas Cherenkov detector reflects how likely it is that a particle exceeded this threshold and produced Cherenkov light. Furthermore, the SHMS Noble Gas Cherenkov detector is useful for e^-/π^- discrimination and its corresponding antipair. In the LD_2^- setting, there are only negative particles present, and the dominant background in the SHMS arm is electrons. Since π^- have a bigger mass and a slower speed than electrons with the same momentum, π^- will produce less signal than electrons in the SHMS Noble Gas Cherenkov detector, because overall it will produce less Cherenkov light. In Figure 22.0(a), before any cuts, there is a dense horizontal band across the top, showing electron events with high photoelectron

counts. After applying the cuts in Figure 13.0, Figure 22.0 panel b) showcases that the electron band is almost entirely removed. What remains is a vertical band at the neutron mass (0.937 $\frac{GeV}{c^2}$), corresponding to true π^- events. For this reason, P.ngcer.npeSum < 2.4 cut was chosen to be applied to all the plots in the LD_2^- and LD_2^+ setting.

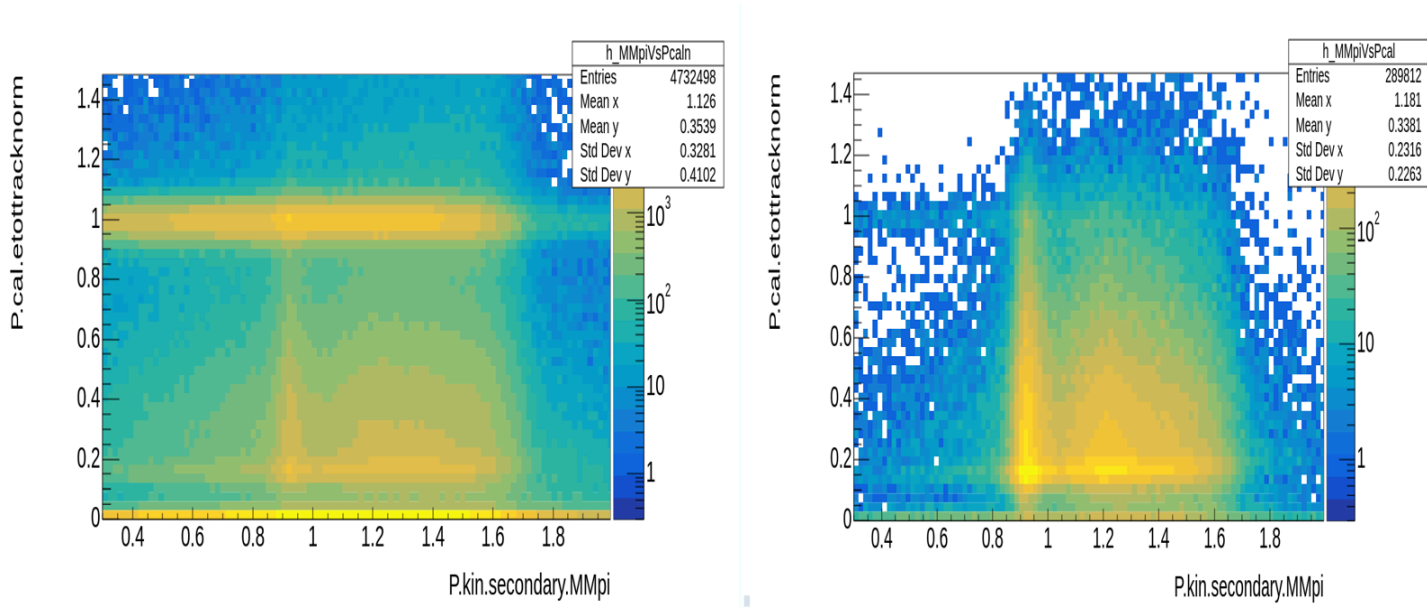

(Figure 23.0)

(a) (b)

Figure 23.0, panels a) and b), represent the MMπ vs. SHMS Calorimeter (P.cal.etottracknorm) plots in the LD_2^- setting. The SHMS Calorimeter is an electromagnetic calorimeter used to measure the energy deposited by charged particles, normalized to their momentum. It plays a key role in particle identification (PID) by distinguishing between electrons and hadrons (such as π^-) based on their energy deposition behaviour. In Figure 23.0 panels a) and b), before any cuts, a dense horizontal band is visible around P.cal.etottracknorm ≈ 1.0, corresponding to electrons. π^-, being hadrons, deposit much less energy relative to their

momentum. Which means the cut must be P.cal.etottracknorm < 1.0, due to this reason P.cal.etottracknorm < 0.8 cut was chosen to be applied to all the plots.

Conclusion

This project focused on the analysis of charged pion electroproduction using data from the LD_2^+ and LD_2^- targets at Jefferson Lab. The primary objective was to isolate clean signals of π^+ and π^- events by applying a series of kinematic and detector-based cuts to reduce background signals from particles such as protons, kaons, and electrons/positrons. A step-by-step methodology was used to develop and apply cuts based on several key detectors in the HMS and SHMS spectrometers. The coincidence time (coin time) cut was first applied to remove random background and retain prompt pion events. The RF time cut was then used to isolate beam-synchronized interactions and refine event selection. These timing cuts ensured that only true coincidence events associated with the beam structure were considered.

For particle identification, a set of carefully chosen cuts was applied to the calorimeter and Cherenkov detectors to isolate π^+. In the LD_2^+ setting, where positrons are present instead of electrons, cuts such as H.cal.etottracknorm > 0.7 (HMS Calorimeter) and H.cer.npeSum > 2.0 (HMS Heavy Gas) were used to suppress heavier hadron backgrounds (protons and kaons). The positron contamination was minimal and did not require significant rejection. In the case of the LD_2^+ setting, cuts such as -2.0 < CTime.ePiCoinTime_ROC1 < 2.0 (Coin Time) and 1.5 < RFTime.SHMS_RFtimeDist < 3.0 (RF time) was used to remove heavier particles such as protons and kaons.

In contrast, the LD_2^- setting required stricter electron rejection, since electrons made up a significant portion of the background. To address this, cuts such as P.cal.etottracknorm < 0.8

(SHMS Calorimeter) and P.ngcer.npeSum < 2.4 (SHMS Noble Gas) were applied. These effectively suppressed the electron background while preserving the π^- signal.

Importantly, the final missing mass distributions for both LD_2^+ and LD_2^- data sets, after all cuts were applied, showed a narrow, well-defined peak at $0.937\frac{GeV}{c^2}$, corresponding to the mass of the neutron. This result confirms that the desired pion production reactions were successfully isolated and that the chosen cuts effectively removed unrelated background signals. Furthermore, the cuts applied to the LD_2^- data were developed in direct comparison with the LD_2^+ results. It is because π^+ and π^- are kinematically symmetric in this reaction that the π signals in both data sets should appear in the same region of missing mass plots. The consistency of the final distributions between LD_2^+ and LD_2^- also validates the reliability of the method.